Transmit Pulse Shaping for 1-Bit GNSS Receivers

Christoph Enneking[(1)], Florian C. Beck[(1)], Steffen Thölert[(1)] and Felix Antreich[(2)]

[(1)]*Institute for Communications and Navigation, German Aerospace Center (DLR)*, Wessling, Germany
[(2)]*Department of Telecommunications, Aeronautics Institute of Technology (ITA)*, São José dos Campos, Brazil
Email: {christoph.enneking,florian.beck,steffen.thoelert}@dlr.de, antreich@ieee.org

***Abstract*—The use of a 1-bit analog-to-digital converter (ADC) with low sampling rate (1-3 MHz) offers a drastic reduction of power consumption for mass-market receivers of the global navigation satellite system (GNSS). Given the low bandwidth of such a front-end, we propose pulse shaping at the satellite to avoid the significant bandlimiting loss currently experienced by the rectangular (REC) pulse. The disadvantages of a non-binary pulse are the reduction of the high power amplifier (HPA) efficiency, and that a 1-bit receiver can neither sample nor replicate the pulse perfectly. Nevertheless, our analytical and numerical results show that there are pulse shapes with a performance gain of 0.3 to 1.1 dB in terms of correlator output signal-to-noise ratio (SNR) compared with the REC pulse, due to lower combined losses of bandlimiting, sampling, quantization, and replica mismatch. We conclude that transmit pulse shaping may be a simple way forward to improve the navigation performance for mass-market GNSS users.**

***Index Terms*—A/D-conversion, snapshot receiver, implementation losses, global positioning system (GPS).**

I. Introduction

Mass-market consumer electronics such as mobile phones, asset trackers, or smartwatches rely more and more on global navigation satellite systems (GNSSs) for location based services (LBS). Such battery-powered devices have often stringent requirements on power and energy consumption, which do not align well with the considerable power demand of the GNSS technology [1]. Galileo Evolution working groups are recognizing the importance of providing signals that economize receiver processing resources [2]. In fact, enabling low power dissipation at the receiver has become an important signal design driver.

One particularly power-hungry element of the GNSS receiver is the analog-to-digital converter (ADC), which converts the analog received signal to a discrete-time and discrete-amplitude digital signal. Virtually all subsequent processing (acquisition, pseudoranging, positioning) could be offloaded to a cloud-based server, which lets A/D-conversion act as a bottleneck in terms of power and energy usage. The ADC's power consumption grows exponentially with the number of bits b used for the signal quantization, as the number of required comparators is 2^b-1. Moreover, the power consumption is proportional to the ADC's sampling rate. Therefore, an appealing option to drastically minimize power consumption is to use an ADC that has 1-bit resolution and low sampling rate (1-3 samples per chip), after applying an appropriate bandlimiting (anti-aliasing) filter [3].

For the receiver front-end just described, are the current GNSS signals in space well-tailored? GNSSs use exclusively the infinite-bandwidth rectangular (REC) pulse, modulated by a binary phase-shift keying (BPSK) or a binary offset carrier (BOC) spreading sequence [4]. Such waveforms assume binary values $\{-1,+1\}$ in theory. This may lead to the intuitive assumption that they should be especially suited for 1-bit A/D-conversion. However, only a fraction of the REC pulse's power passes through the anti-aliasing filter. For instance, passing a BPSK-REC (a.k.a. BPSK-R) waveform through a "brick-wall" filter with two-sided bandwidth equal to the keying rate leads to a -1.1 dB (23%) bandlimiting loss. Transmit pulse shaping, i.e., changing the waveform to an effectively bandlimited signal at the satellite, would avoid this loss and has been proposed for GNSS in the 2000s [5]–[7], but this option was discarded in the development phase of Galileo. The decision in favor of rectangular signaling seems to have been a compromise to serve many different user groups with different performance demands and front-end bandwidths. Some of the pros and cons of transmit pulse shaping for GNSS and the historical background of the decision at that time are summarized in [8]. However, we may see a resurgence of this debate, given that the rapid growth of the consumer GNSS user segment was not foreseeable in the early 2000s.

In this work, we revisit two frequent arguments against pulse shaping and put them to the test. Firstly, it is often believed that non-binary waveforms cannot be processed or replicated effectively by 1-bit receivers, the intuition being that they cannot be reconstructed perfectly from digital samples. Secondly, non-binary waveforms often have a high peak-to-average power ratio (PAPR), which can lead to inefficient operation of the satellite's high power amplifier (HPA) [9]. Note that there are many other aspects of pulse shaping which must be considered before deciding for a new signal design (autocorrelation shape, multipath susceptibility, jamming protection, radio frequency compatibility, etc.), but these are beyond the scope of this contribution.

Specifically, we compare the achievable signal-to-noise ratio (SNR) of 1 ms prompt-correlation sums for several candidate pulse shapes, as experienced with a 1-bit ADC output after correlation with a 1-bit replica. We assume that the ideal modulated pulse is amplified by a given HPA under either

978-1-6654-0575-1/22/$31.00 ©2022 IEEE

a maximum or average TX power constraint. We quantify the performance via numerical simulations and analytically, using known results from [10]–[14] to compute implementation losses due to bandlimiting, sampling, and quantization (BSQ). For the special case of 1-bit resolution, the extended Bussgang decomposition [15] and the celebrated arcsine law [16] allow for very compact performance expressions. Results suggest that raised cosine (RC), sinc or Gaussian pulses can outperform the REC pulse shape by 0.3 to 1.1 dB.

II. System Model

We consider the system shown in Fig. 1, consisting of transmitter (TX), channel, and receiver (RX) elements. The RX described here uses 1-bit ADC resolution and 1-bit resolution of the local replica (1-bit/1-bit).

A. Analog Transmit and Receive Signal

We start with a binary impulse train

$$b(t) = \sum_{m=-\infty}^{\infty} b[m]\delta(t - mT_c), \tag{1}$$

where $b[m]$ is a BPSK spreading sequence $b[m] \in \{+1, -1\}$, $\delta(t)$ is the Dirac impulse, and the chip rate is set to $1/T_c = 1.023$ MHz. We assume that $b[m]$ repeats after N_c chips, i.e., $b(t)$ has period $T = N_c T_c$. The analog pulse shape is denoted by $h(t) \in \mathbb{R}$, which need not be a REC pulse and will be specified in Section V-A. The pulse-shaped navigation signal

$$c(t) = \sum_{m\in\mathbb{Z}} b[m]h(t - mT_c) \tag{2}$$

is multiplied by a carrier $\sqrt{2}\cos(\omega t + \theta_0)$ with angular frequency ω and phase θ_0. The resulting bandpass signal $x(t)$ is input to an HPA. The amplifier is modeled as a memoryless soft-limiter with input-output relationship

$$y(t) = \begin{cases} -A_0 & x(t) \le -x_0 \\ \gamma x(t) & -x_0 < x(t) \le x_0 \\ A_0 & x(t) > x_0. \end{cases} \tag{3}$$

This HPA clips all input amplitudes larger than a certain threshold x_0 to have amplitude $A_0 = \gamma x_0$, but is otherwise distortion-free. The first zonal bandpass filter $h_o(t)$ rejects harmonics of the nonlinearly distorted signal at $0\omega_c, 2\omega_c, 3\omega_c, \ldots$ [17]. The result is a radio signal $z(t)$.

The radio signal is propagated through an additive white Gaussian noise (AWGN) delay channel with time delay $\tau_0 \in [0, T_c)$, gain G and AWGN $\eta(t)$ with two-sided power spectral density (PSD) $N_0/2$.

At the receiver, the signal is demodulated from the carrier, using a phase estimate θ, and filtered by a lowpass filter (LPF) with impulse response $h_r(t)$. We assume an ideal "brick-wall" filter with two-sided bandwidth $B = 1.023$ MHz. The analog receive signal after downconversion and filtering is given by

$$r(t) = s(t - \tau_0) + n(t), \tag{4}$$

where $s(t-\tau_0)$ is a distorted and delayed version of $c(t)$, while $n(t)$ is bandlimited AWGN with autocorrelation function

$$\mathrm{E}\left[n(t)n(t+\epsilon)\right] = \frac{N_0}{2}\frac{\sin(\pi B\epsilon)}{\pi\epsilon}. \tag{5}$$

B. A/D-Conversion and Correlation With Local Replica

Collecting N samples at a rate of $1/T_s$ and converting to 1-bit resolution leads to the ADC output

$$r[n] = \mathrm{sgn}\left(r(nT_s)\right) \tag{6}$$

for $n = 1, \ldots, N$, where we used the signum function

$$\mathrm{sgn}(x) = \begin{cases} +1 & x \ge 0 \\ -1 & x < 0. \end{cases} \tag{7}$$

The local replica is assumed to be a sampled version of the ideal signal $c(t)$ with 1-bit resolution

$$c[n;\tau] = \mathrm{sgn}\left(c(nT_s - \tau)\right), \tag{8}$$

where $\tau \in \mathbb{R}$ denotes an estimate of the signal delay. An integrate and dump (I&D) filter finally leads to the prompt correlator output

$$P(\tau, \theta) = \sum_{n=1}^{N} c[n;\tau]r[n], \tag{9}$$

parameterized by the estimates τ and θ.

C. Matrix-vector Notation

We introduce the vector of ADC output samples

$$\boldsymbol{r}' = \left[r[1] \ \ldots \ r[N]\right]^T \quad \in \{-1, +1\}^N \tag{10}$$

and the vector of continuous-valued samples

$$\boldsymbol{r} = \left[r(T_s) \ \ldots \ r(NT_s)\right]^T \quad \in \mathbb{R}^N. \tag{11}$$

Furthermore, let

$$\boldsymbol{s}(\tau_0) = \left[s(T_s - \tau_0) \ \ldots \ s(NT_s - \tau_0)\right]^T \tag{12}$$

$$\boldsymbol{n} = \left[n(T_s) \ \ldots \ n(NT_s)\right]^T \tag{13}$$

so that

$$\boldsymbol{r} = \boldsymbol{s}(\tau_0) + \boldsymbol{n}. \tag{14}$$

The noise is Gaussian distributed $\boldsymbol{n} \sim \mathcal{N}(\boldsymbol{0}, \sigma^2\boldsymbol{W})$, with variance $\sigma^2 = BN_0/2$ and a matrix accounting for the correlation of noise samples

$$[\boldsymbol{W}]_{ij} = \mathrm{sinc}\left(B(i-j)T_s\right), \qquad i, j = 1, \ldots, N. \tag{15}$$

The sinc function is defined as $\mathrm{sinc}(x) = \sin(\pi x)/(\pi x)$ if $x \neq 0$ and $\mathrm{sinc}(0) = 1$. We also introduce the sampled and delayed version of the ideal signal

$$\boldsymbol{c}(\tau) = \left[c(T_s - \tau) \ c(2T_s - \tau) \ \ldots \ c(NT_s - \tau)\right]^T. \tag{16}$$

Then, the I&D filter output can be written as

$$P(\tau, \theta) = \mathrm{sgn}\left(\boldsymbol{c}^T(\tau)\right)\boldsymbol{r}'. \tag{17}$$

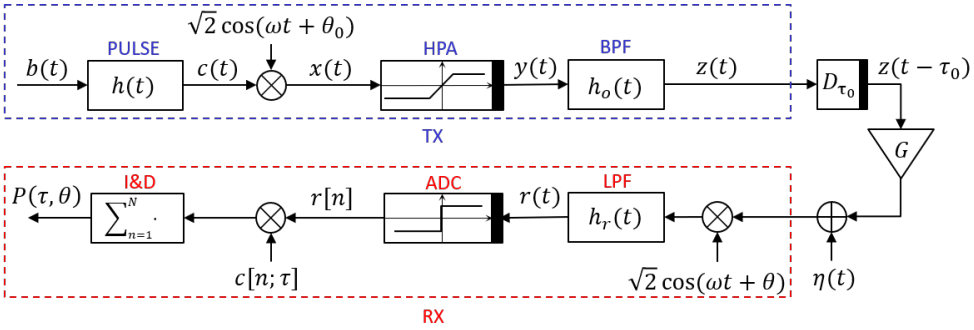

Fig. 1: Transmit (TX) and receive (RX) signal processing. Nonlinearities (HPA, ADC, and delay operator D_{τ_0}) are indicated by a black bar.

III. Bussgang Decomposition of Noisy 1-bit Signal

Using the extended Bussgang decomposition [15], we may write the ADC output as the sum

$$\boldsymbol{r}' = \boldsymbol{s}'(\tau_0) + \boldsymbol{n}' \tag{18}$$

of a useful signal

$$\boldsymbol{s}'(\tau_0) = \sqrt{\frac{2}{\pi}}\frac{\boldsymbol{s}(\tau_0)}{\sigma} \tag{19}$$

and a random vector that can be approximated as zero-mean correlated Gaussian noise

$$\boldsymbol{n}' \sim \mathcal{N}(0, \boldsymbol{W}'). \tag{20}$$

As the pre-correlation SNR is low for GNSS, we have $\mathrm{E}[\boldsymbol{r}\boldsymbol{r}^T] \approx \mathrm{E}[\boldsymbol{n}\boldsymbol{n}^T]$ and we can apply the arcsine law [16] to calculate the noise covariance matrix

$$\boldsymbol{W}' = \frac{2}{\pi}\arcsin(\boldsymbol{W}). \tag{21}$$

Note that this version of the Bussgang decomposition is an approximate probabilistic description of the ADC output, which should only be used at low SNR. It has been used in related works [13], [14].

IV. Effective C/N_0

As performance metric, we consider the effective C/N_0, following the definition of Betz [4], [18]. To this end, we first define the coherent output SNR as the ratio of squared mean and variance

$$\rho = \frac{\left(\mathrm{E}\left[P(\tau_0,\theta_0)\right]\right)^2}{\mathrm{Var}\left[P(\tau_0,\theta_0)\right]} \tag{22}$$

for the case that delay and phase estimate are perfect, that is $\tau = \tau_0$ and $\theta = \theta_0$, respectively. The effective C/N_0 is just a scaled version of the coherent output SNR

$$\left(\frac{C}{N_0}\right)_{\mathrm{eff}} = \frac{\rho}{2NT_s}, \tag{23}$$

to avoid dependency on the coherent averaging time NT_s.

The coherent output SNR can be calculated with (17)-(21)

$$\rho = \frac{1}{\sigma^2}\frac{\left(\mathrm{sgn}\left(\boldsymbol{c}^T(\tau_0)\right)\boldsymbol{s}\right)^2}{\mathrm{sgn}\left(\boldsymbol{c}^T(\tau_0)\right)\arcsin(\boldsymbol{W})\,\mathrm{sgn}\left(\boldsymbol{c}(\tau_0)\right)}. \tag{24}$$

In addition to the above, we consider also the SNR that can be achieved if the resolution of either the ADC, the local replica, or both, are not 1-bit but ∞-bit. Accordingly, the hard-limiting operations in (6) and/or (8) are omitted. This leads to a total of four cases, whose respective coherent output SNRs we indicate with sub-/superscripts as follows:

- 1-bit ADC resolution, 1-bit replica: ρ
- 1-bit ADC resolution, ∞-bit replica: $\rho^{(\infty)}$
- ∞-bit ADC resolution, 1-bit replica: ρ_∞
- ∞-bit ADC resolution, ∞-bit replica: $\rho_\infty^{(\infty)}$.

The coherent output SNRs of the latter three are given as

$$\rho^{(\infty)} = \frac{1}{\sigma^2}\frac{\left(\boldsymbol{c}^T(\tau_0)\boldsymbol{s}\right)^2}{\boldsymbol{c}^T(\tau_0)\arcsin(\boldsymbol{W})\boldsymbol{c}(\tau_0)} \tag{25}$$

$$\rho_\infty = \frac{1}{\sigma^2}\frac{\left(\mathrm{sgn}\left(\boldsymbol{c}^T(\tau_0)\right)\boldsymbol{s}\right)^2}{\mathrm{sgn}\left(\boldsymbol{c}^T(\tau_0)\right)\boldsymbol{W}\,\mathrm{sgn}\left(\boldsymbol{c}(\tau_0)\right)} \tag{26}$$

$$\rho_\infty^{(\infty)} = \frac{1}{\sigma^2}\frac{\left(\boldsymbol{c}^T(\tau_0)\boldsymbol{s}\right)^2}{\boldsymbol{c}^T(\tau_0)\boldsymbol{W}\boldsymbol{c}(\tau_0)}. \tag{27}$$

A well-known result is that the quantization loss introduced by the ADC's hard-limiting operation is

$$\frac{\rho^{(\infty)}}{\rho_\infty^{(\infty)}} = \frac{\boldsymbol{c}^T(\tau_0)\boldsymbol{W}\boldsymbol{c}(\tau_0)}{\boldsymbol{c}^T(\tau_0)\arcsin(\boldsymbol{W})\boldsymbol{c}(\tau_0)} = \Big|_{\boldsymbol{W}=\boldsymbol{I}} = \frac{2}{\pi} \tag{28}$$

in the special case of Nyquist sampling, where $\boldsymbol{W}$ becomes the identity matrix $\boldsymbol{I}$. Note that $2/\pi$ corresponds to -1.96 dB.

The above SNR expressions show, however, that there is also a loss due to the use of a 1-bit replica. For instance, using 1-bit resolution for the ADC and for the replica leads to a loss compared with an ideal ∞-bit system of

$$\frac{\rho}{\rho_\infty^{(\infty)}} = \frac{\boldsymbol{c}^T(\tau_0)\boldsymbol{W}\boldsymbol{c}(\tau_0)}{\mathrm{sgn}\left(\boldsymbol{c}^T(\tau_0)\right)\arcsin(\boldsymbol{W})\,\mathrm{sgn}\left(\boldsymbol{c}(\tau_0)\right)} \times \left(\frac{\mathrm{sgn}\left(\boldsymbol{c}^T(\tau_0)\right)\boldsymbol{s}}{\boldsymbol{c}^T(\tau_0)\boldsymbol{s}}\right)^2. \tag{29}$$

V. Numerical Results

Simulations are performed for a number of specific pulse shape candidates, to be specified next. The performance results depend critically on the operating region of the HPA, so that

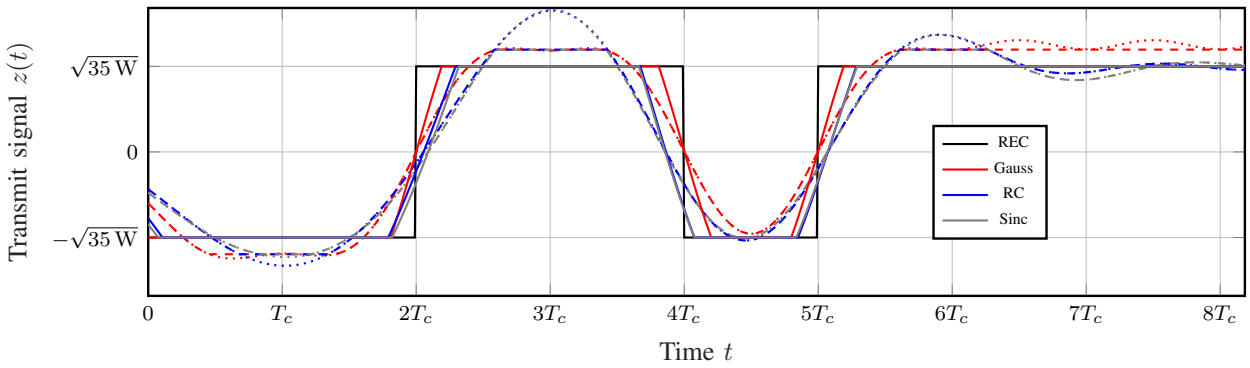

Fig. 2: Short segment of the transmit signal for different pulse shapes and HPA operation regions. Solid: saturation region; dashed: transition region; dotted: linear region. (Envelope only, carrier removed for clarity.)

we dedicate a short section on possible scenarios in this regard, before presenting the actual results.

A. Pulse Shapes

The following four specific pulse shapes $h(t)$ will be investigated:

1) a REC pulse as used by GNSS

$$h(t) = \begin{cases} 1 & |t/T_c| \le 1/2 \\ 0 & \text{otherwise;} \end{cases} \tag{30}$$

2) a Gaussian pulse with $\sigma^2 = 0.195$

$$h(t) = \frac{1}{\sqrt[4]{\pi\sigma^2}} e^{-\frac{1}{2\sigma^2}\frac{t^2}{T_c^2}}, \tag{31}$$

as used with Gaussian minimum shift keying (GMSK) in GSM ("time-bandwidth product 0.3") [19];

3) a RC pulse with roll-off factor $\alpha = 0.22$

$$h(t) = \frac{\mathrm{sinc}(t/T_c)}{\sqrt{1-\alpha/4}} \frac{\cos(\pi\alpha t/T_c)}{1-(2\alpha t/T_c)^2} \tag{32}$$

as used in UMTS [20], [21];

4) a sinc pulse (equivalent to a RC pulse with $\alpha = 0$)

$$h(t) = \mathrm{sinc}(t/T_c), \tag{33}$$

as used in the IS-95 standard [22].

It is easily checked that $\int_{-\infty}^{\infty} h^2(t)\,\mathrm{d}t = T_c$ for all pulse shapes. Therefore, the resulting navigation signal $c(t)$ has unit average power, i.e., $\frac{1}{T}\int_T c^2(t)\,\mathrm{d}t = 1$ for any integration interval of duration equal to the signal period T. The PAPR is thus given by

$$\mathrm{PAPR} = \max_{t\in[0,T)} c^2(t)/1. \tag{34}$$

With the above pulses, we observed a PAPR of, respectively,

$$0\,\mathrm{dB} \quad / \quad 2.31\,\mathrm{dB} \quad / \quad 6.20\,\mathrm{dB} \quad / \quad 7.89\,\mathrm{dB}.$$

B. Assumptions on the HPA

Unfortunately for signal design research, little is known publicly about the true amplifier characteristics in GNSS (and how much leeway there is left in terms of maximum output power). This is why we consider the following three scenarios:

1) *Linear region* ($\gamma \ll A_0$):
   e.g., $\gamma^2 = 35$ W, $A_0^2 = 250$ W (8.5 dB input backoff).
2) *Transitition region* ($\gamma \approx A_0$):
   e.g., $\gamma^2 = 35$ W, $A_0^2 = 50$ W (1.5 dB input backoff).
3) *Saturation region* ($\gamma > A_0$):
   e.g., $\gamma^2 = 110$ W, $A_0^2 = 35$ W (5 dB compression point).

The HPA output envelope for all scenarios and pulses is shown in Fig. 2. All three scenarios lead to an HPA output envelope with average power $P_0 \triangleq \min(A_0^2, \gamma^2) = 35\,\mathrm{W}$. The convenience of the REC pulse is that the HPA produces an undistorted output envelope, irrespective of its operation region. The same would be true for all navigation signals with constant envelope $|c(t)| \equiv 1$ (i.e., PAPR equal to 0 dB). For all other pulse shapes considered, various degrees of clipping can be observed, which will indeed affect the performance.

C. Performance Comparison and Discussion

Performance results for the three amplifier scenarios are shown in Figs. 3-5 as a function of sampling rate. Recall that the receive bandwidth is fixed at $B = 1.023\,\mathrm{MHz}$, so that sampling rates $1/T_s > B$ represent oversampling. Lines represent the analytical results from the expressions (24)-(27), while markers represent software simulation results of the TX/RX system shown in Fig. 1. A large number of Monte Carlo runs (10^4) was performed to randomize over AWGN, and over the time offset $\tau_0 \in [0, T_c)$ to eliminate the dependency of performance on the phasing of sample epochs with respect to signal transitions [11]. We used a coherent integration time equal to the code period $NT_s = T = 1\,\mathrm{ms}$. For the channel gain G (including TX antenna gain and free-space/atmospheric loss), we use $-174\,\mathrm{dB}$. The noise floor N_0 for a mass-market receiver is assumed at $-201.5\,\mathrm{dBW/Hz}$. Thus, $P_0G^2/N_0 = 42.9\,\mathrm{dB\text{-}Hz}$ serves as an upper bound on the achievable effective C/N_0. From the results, we make the following observations:

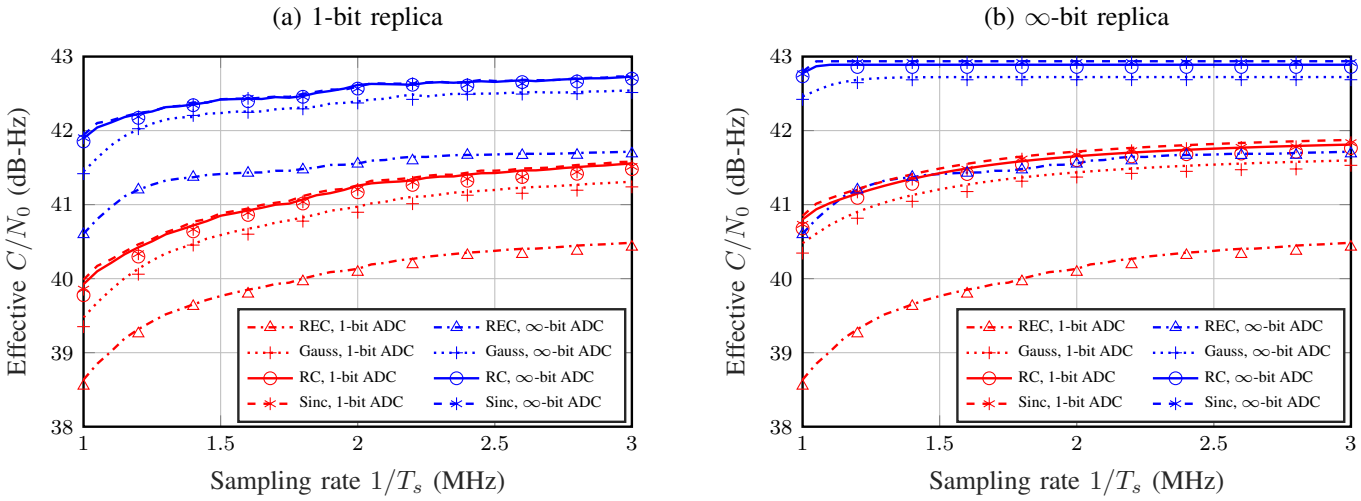

Fig. 3: Effective C/N_0 for HPA operating in linear region. Markers: simulated; lines: analytical.

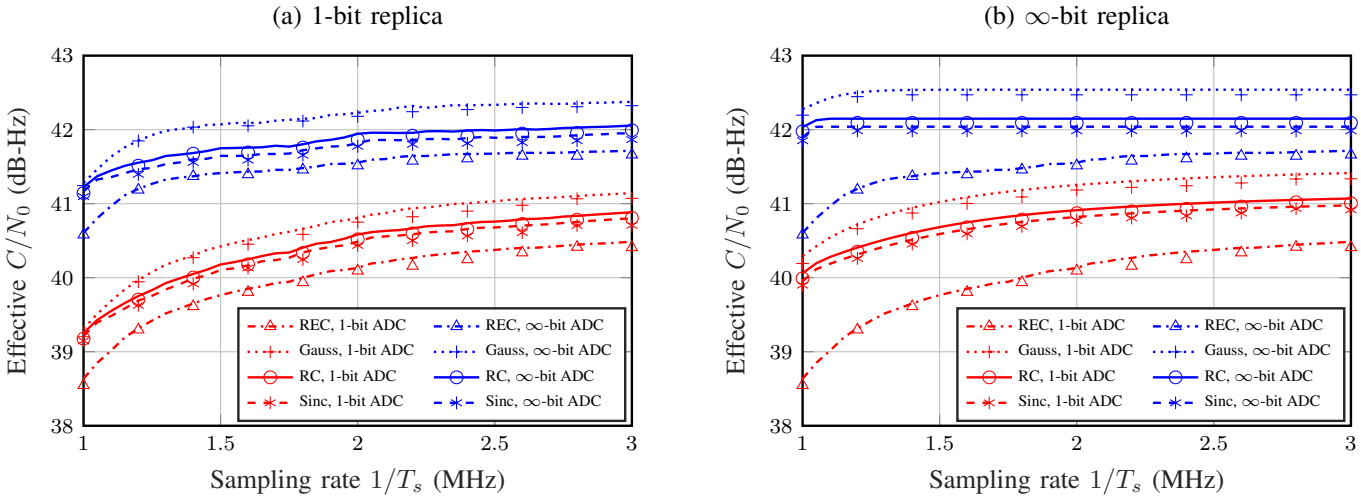

Fig. 4: Effective C/N_0 for HPA operating in transition region. Markers: simulations; lines: analytical.

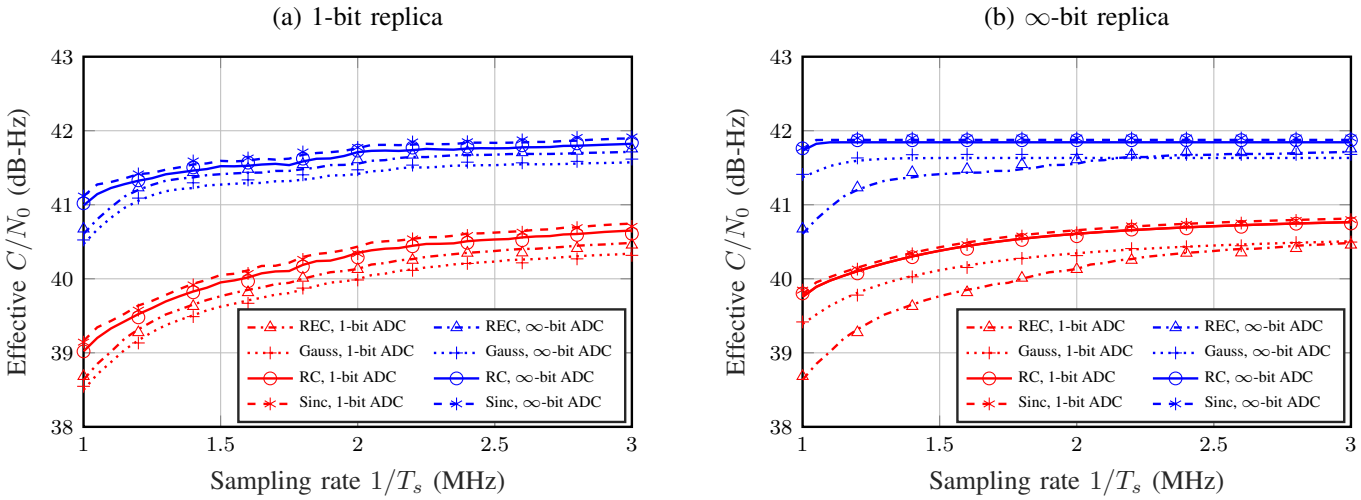

Fig. 5: Effective C/N_0 for HPA operating in saturation region. Markers: simulations; lines: analytical.

- The curves "REC, 1-bit ADC" and "REC, ∞-bit ADC" are identical over all six plots, as expected. They do not depend on the HPA operating region, ADC resolution or replica resolution.
- If the HPA operates in the linear region, the advantage of pulse shaping is most significant: all pulses attain the same TX power of $35\,\mathrm{W}$, but not all are equally affected by the receiver's LPF. Bandlimitation leads to a signficant $1.1\,\mathrm{dB}$ loss of the REC pulse, for instance. This explains why essentially bandlimited pulses outperform the REC (by $1.1\,\mathrm{dB}$ in case of sinc, $0.82\,\mathrm{dB}$ in case of Gaussian pulse, in terms of the 1-bit/1-bit performance ρ).
- In the HPA's transition region, clipping and spectral regrowth of previously bandlimited signals lead to a reduction of the pulse shaping gain. Still, the REC pulse is the worst option, being outperformed by the Gaussian pulse by $0.66\,\mathrm{dB}$ and by the sinc pulse by $0.32\,\mathrm{dB}$.
- If the HPA operates in saturation, the transmitted signals approach a rectangular waveform and the performance of all pulse options is similar. Nevertheless, especially at low sampling rates, RC and sinc pulse still outperform the REC pulse by 0.3 to $0.5\,\mathrm{dB}$. Note from Fig. 2 that their chip transitions are less steep and can better pass the LPF.
- The 1-bit quantization loss of ADC and replica can both be reduced by oversampling. This is well-known for the ADC loss (reduction from $1.96\,\mathrm{dB}$ to $1.2\,\mathrm{dB}$ for $3\,\mathrm{MHz}$), but perhaps a bit surprising for the replica loss (the second factor in (29), reduction from $1.0\,\mathrm{dB}$ to $0.3\,\mathrm{dB}$).
- The RC and sinc pulse outperform the REC pulse in all HPA scenarios and for all receiver configurations, including the 1-bit ADC/1-bit replica case.
- The Gaussian pulse, which is neither timelimited nor bandlimited in theory, appears to achieve a good tradeoff between spectral concentration and HPA efficiency in the HPA transition region.
- For all the considered HPA scenarios, the REC is the worst option (with one minor exception in Fig. 5a where the Gaussian pulse performs $0.1\,\mathrm{dB}$ poorer).

VI. Conclusion

We argued that 1-bit GNSS receivers (with 1-bit ADC resolution and 1-bit local signal replica) are a power-efficient option for mass-market user categories. However, we showed that such a low-cost implementation can come with a severe performance penalty, owing to the losses of BSQ and replica mismatch. With the currently used REC pulse shape of GNSS signals, much of these losses is due to the receiver's anti-aliasing LPF. Transmit pulse shaping can achieve a better trade-off in terms of overall losses, with a gain of 0.3 to 1.1 dB depending on the HPA operating region and receiver sampling rate. The pulse shaping can be done on the TX side only, without the need for any major RX hardware modifications. Our performance analysis here was limited to the peak value of post-correlation SNR. It is well-known that the the positioning accuracy also depends on the shape (sharpness) of the correlation function, which of course depends on the pulse shape. The investigation of these effects on low-complexity receivers is subject of our ongoing work [23] and future work.

References

[1] "Power-efficient positioning for the Internet of Things: merging GNSS with low power connectivity solutions: white paper," European GNSS Agency, Publications Office of the EU, Tech. Rep., 2020.

[2] S. Wallner *et al.*, "Novel Concepts on GNSS Signal Design serving Emerging GNSS User Categories: Quasi-Pilot Signal," in *2020 European Navigation Conference (ENC)*, Nov. 2020, pp. 1–22.

[3] A. Kumari and D. Bhatt, "Advanced system analysis and survey on the GPS receiver front end," *IEEE Access*, vol. 10, pp. 24 611–24 626, 2022.

[4] J. W. Betz, *Engineering Satellite-Based Navigation and Timing: Global Navigation Satellite Systems, Signals, and Receivers*. John Wiley & Sons, Dec. 2015.

[5] R. Schweikert, T. Wörz, R. De Gaudenzi, A. Steingass, and A. Dammann, "On signal structures for GNSS-2," *International Journal of Satellite Communications*, vol. 18, no. 4-5, pp. 271–291, 2000.

[6] M. Quinlan, G. Burden, S. Rollet, R. De Gaudenzi, and S. Harding, "Validation of novel navigation signal structures for future GNSS systems," in *Position location and navigation symposium (PLANS)*, Apr. 2004, pp. 389–398.

[7] F. Antreich and J. A. Nossek, "Optimum chip pulse shape design for timing synchronization," in *2011 IEEE international conference on acoustics, speech and signal processing (ICASSP)*, May 2011, pp. 3524–3527.

[8] J.-A. Avila-Rodriguez, "On Generalized Signal Waveforms for Satellite Navigation," Ph.D. dissertation, University of the Federal Armed Forces (UFAF) Munich, Jun. 2008.

[9] C. Rapp, "Effects of HPA-nonlinearity on 4-DPSK/OFDM-signal for a digital sound broadcasting system," in *Proceedings of the 2nd European Conference on Satellite Communication*, Oct. 1991, pp. 179–184.

[10] J. W. Betz and N. R. Shnidman, "Receiver Processing Losses with Bandlimiting and One-Bit Sampling," in *Proceedings of the 20th International Technical Meeting of the Satellite Division of The Institute of Navigation (ION GNSS 2007)*, Sep. 2007, pp. 1244–1256.

[11] C. Hegarty, "Analytical model for GNSS receiver implementation losses," *NAVIGATION: Journal of the Institute of Navigation*, vol. 58, pp. 29–44, Mar. 2011.

[12] M. S. Stein, "Signal Parameter Estimation with 1-bit ADC," Dissertation, Technische Universität München, München, 2016.

[13] F. Wendler, M. Stein, A. Mezghani, and J. Nossek, "Quantization-loss reduction for 1-bit BOC positioning," in *Proceedings of the 2013 International Technical Meeting of The Institute of Navigation*, Jan. 2013, pp. 509–518.

[14] M. Stein, F. Wendler, A. Mezghani, and J. A. Nossek, "Quantization-loss reduction for signal parameter estimation," in *2013 IEEE International Conference on Acoustics, Speech and Signal Processing*, May 2013, pp. 5800–5804.

[15] O. T. Demir and E. Bjornson, "The Bussgang Decomposition of Nonlinear Systems: Basic Theory and MIMO Extensions [Lecture Notes]," *IEEE Signal Processing Magazine*, vol. 38, no. 1, pp. 131–136, Jan. 2021.

[16] J. Van Vleck and D. Middleton, "The spectrum of clipped noise," *Proceedings of the IEEE*, vol. 54, no. 1, pp. 2–19, Jan. 1966.

[17] N. Blachman, "Band-pass nonlinearities," *IEEE Transactions on Information Theory*, vol. 10, no. 2, pp. 162–164, Apr. 1964.

[18] J. W. Betz and K. R. Kolodziejski, "Generalized theory of code tracking with an early-late discriminator part I: Lower bound and coherent processing," *IEEE Transactions on Aerospace and Electronic Systems*, vol. 45, no. 4, pp. 1538–1556, Oct. 2009.

[19] "Bandwidth-Efficient Modulations," Consultative Committee for Space Data Systems (CCSDS), Washington, D. C., USA, Informational Report Issue 2, Oct. 2009.

[20] "Radio Transmission and Reception," European Telecommunications Standards Institute, Tech. Rep. ETSI TS 125 102, V3.1.0, Jan. 2000.

[21] J. G. Proakis, *Digital Communications*. McGraw-Hill, 2001.

[22] J. S. Lee and L. E. Miller, *CDMA Systems Engineering Handbook*. Artech House, 1998.

[23] F. C. Beck, C. Enneking, S. Thoelert, and F. Antreich, "Comparison of Constant and Non-constant Envelope Signals for Satellite Navigation," in *NAVITEC 2022 Signal Workshop*, Apr. 2022.